Eigenmode Analysis of Geodesic Acoustic Mode and Zonal Flow

Zhe Gao 1), K. Itoh 2), H. Sanuki 2), and J. Q. Dong 3)

1) Department of Engineering Physics, Tsinghua University, Beijing 100084, PR China
2) National Institute for Fusion Science, Toki, Gifu 509-5292, Japan
3) Southwestern Institute of Physics, Chengdu 610041, PR China

email contact of main author: gaozhe@tsinghua.edu.cn

Abstract. We employ a linear gyrokinetic model in collisionless toroidal plasmas with an electrostatic potential nearly constant around a magnetic surface, and then the plasma response is analytically solved. Besides the trivial zero frequency solution and the standard GAM solution, a branch of low frequency mode and an infinite series of ISW-like modes are found. The ISW-like modes are strongly damped. For a low electron/ion temperature ratio, τ , the low frequency eigenmode has a rigid zero frequency in the low q region but oscillates with a finite frequency in the high q region. The critical value of q increases and the finite frequency decreases with an increasing τ . Until τ is larger than 0.55, the mode has a rigid zero frequency for all q. This low frequency eigenmode relaxes on time scaling with the order of transit frequency.

1. Introduction

It is widely accepted [1] that there are two types of zonal flows (ZFs): one is low/zero frequency branch; the other is higher frequency oscillation, so called the geodesic acoustic mode (GAM) [2]. ZFs are believed to be driven by micro-turbulence, and thus moderate turbulence and turbulent transport. However, both the low frequency ZF and GAM, first and foremost, are plasma eigenmodes. The progress of the experimental research on GAM has shown that multiple eigenmodes of GAM coexist simultaneously. [3, 4] This stimulates the research on various types of branches in the family of zonal flows.

The origin of ZFs is the compressibility of poloidal $\mathbf{E}\times\mathbf{B}$ flow. If the compression is fully compensated by a parallel return flow, it gives a zero frequency ZF; [5] while, if the compression mostly induces a temporal oscillation of density and only a little part is compensated by parallel flow, it gives the standard GAM. [2] When the compensated parallel flow is offered by distributed thermal velocity of particles, the GAM will be damped by the Landau-type collisionless mechanism due to the coupling of the $m=n=0$ $\mathbf{E}\times\mathbf{B}$ flow to the parallel ($m=1/n=0$) flow. However, this kinetic effect may induce multiple eigenmodes. In this work, we solve analytically the linear response of plasma to an electrostatic potential which is nearly constant around a magnetic surface in large aspect ratio axisymmetric toroidal plasmas and report a series of ZF eigenmodes. Among them, there are the standard GAM, a branch of low frequency eigenmode and an infinite series of ISW-like eigenmodes. The relation of this low frequency eigenmode and the stationary zonal flow [6] is also discussed.

2. Governing Equation

For simplicity, we consider a simple axisymmetric toroidal system with the standard model magnetic field, given by $\mathbf{B} = B_0\{[1/(1+\varepsilon\cos\theta)]\mathbf{e}_\varphi + (\varepsilon/q)\mathbf{e}_\theta\}$, where φ and θ are the toroidal and poloidal angles and the inverse aspect ratio $\varepsilon = r/R$ is assumed to be small. If the electrostatic potential ϕ can be decomposed as $\phi = \sum_{\omega,k}\hat{\phi}\exp[ik(r-r_0)-i\omega t]$, the k component of perturbed distribution function $\hat{f}$ can be described as $\hat{f}_j = -q_j F_{0j}\hat{\phi}/T_j + \hat{h}_j J_{0j}$, where the equilibrium distribution F_{0j} is chosen to be Maxwellian at temperature T_j, $J_0 = J_{0j}(k\rho_j)$ is a Bessel function, $\rho_j = v_{\perp j}/\Omega_j$ is the gyroradius and $\Omega_j = q_j B/(m_j c)$ is the gyrofrequency. The nonadiabatic response $\hat{h}_j$ satisfies the linear gyrokinetic equation

$$\left(\omega - \omega_{dj}\sin\theta + i\omega_{tj}\frac{\partial}{\partial\theta}\right)\hat{h}_j = \frac{q_j F_{0j}}{T_j}\omega J_{0j}\hat{\phi}, \tag{1}$$

where $\omega_t = v_{//}/(qR)$ and $\omega_d = k[(2v_{//}^2 + v_\perp^2)/(2\Omega R)]$.

Under the assumption of $\hat{\phi} - \langle\hat{\phi}\rangle << \langle\hat{\phi}\rangle$, where $\langle\hat{\phi}\rangle$ and $\hat{\phi} - \langle\hat{\phi}\rangle$ are the flux surface average of the potential and the poloidal variation from it, the solution of $\hat{f}_i$ can be analytically given as

$$\hat{f}_i = -\frac{q_i F_{0i}\langle\hat{\phi}\rangle}{T_i}\left[1 - J_0^2\sum_{m=-\infty}^{+\infty}\sum_{n=-\infty}^{+\infty} i^{m-n}e^{i(m-n)\theta}\frac{\omega J_m J_n}{\omega + n\omega_{ti}}\right], \tag{2}$$

where $J_{m,n} = J_{m,n}(\omega_{di}/\omega_{ti})$ and the Bessel function expansion $e^{ia\cos\theta} = \sum_{n=-\infty}^{+\infty} i^n J_n(a)\exp(in\theta)$ is used. From Eq. (2), we can see the ion distribution function response, or the density response, includes the components with different θ dependence. Under the assumption of $k\rho_i q << 1$, the constant component over the flux surface, $\hat{f}_{i|m=0}$, is of the order $k^2\rho_i^2 q^2$, the $m=1$ component, $\hat{f}_{i|m=1}$, is of the order $k\rho_i q$, and the $m=2$ component, $\hat{f}_{i|m=2}$, is of the order $k^2\rho_i^2 q^2$, respectively. Since we can assume $k\rho_e \to 0$, the electron response to $\langle\phi\rangle$ is zero, then the poloidal variation of ϕ can not be ignored for electrons. For the $m=1$ potential, the electron response is approximately given by the Boltzmann relation $\hat{f}_{e|m=1} = (eF_{0e}/T_e)\hat{\phi}_{m=1}$. From the quasineutrality condition for $m=1$, the poloidal variation is associated with the ion response to the $m=0$ potential, i.e. $\hat{\phi}_{m=1} = (q_i T_e/n_{0e}e^2)\int d^3v\hat{f}_{i|m=1}$.[7] Then, the electron distribution function can be expressed as

$$\hat{f}_{e|m=1} = (q_i F_{0e}/n_{0e}e)\int d^3v\hat{f}_{i|m=1}. \tag{3}$$

Other $m\neq 0$ components of the electron response can be obtained in the same way, respectively.

The quasineutrality condition for $m=0$, or its flux surface average, offers the governing equation. We can write this condition as $\nabla\cdot\mathbf{j} \sim \langle j_r\rangle = 0$, where $\mathbf{j}$ is the perturbed current including the current due to curvature drift and the polarization current and j_r is its radial component. The equation is described as

$$\int Rd\theta d^3v\left(q_i\hat{f}_i v_{di}\sin\theta - e\hat{f}_e v_{de}\sin\theta - q_i v_p F_0\right)=0\,. \tag{4}$$

Here, $v_{dj}=\omega_{dj}/k$ is the curvature drift velocity, and $v_p = g\omega k\left\langle\hat{\phi}\right\rangle/\left(\Omega_i B_i\right)$ is the polarization drift velocity and $g\approx\left[1-\Gamma_0(b_i)\right]/b_i$ is representing the finite Larmor radius effect to the polarization current. (Note that there is a trivial solution, $\omega\equiv\omega_r - i\gamma = 0$, which corresponds to the zonal flow in the analysis of Rosenbluth-Hinton in the collisionless limit [8]. We here look for the solution with $|\omega|\neq 0$.) Under the assumption of large aspect ratio, only the $m=1$ term contributes to the curvature drift driven current, so Eq. (4) is rewritten as

$$\int_L \frac{d^3v\exp\left(-v^2\right)}{\pi^{3/2}} J_0^2(kv_\perp)\sum_{n=1}^{+\infty} J_n^2\left(kq\frac{v_{//}^2+v_\perp^2/2}{v_{//}}\right)\left(\frac{v_{//}}{\zeta/n-v_{//}}+\frac{-v_{//}}{\zeta/n+v_{//}}\right)\left(1+\frac{\tau}{v_{//}^2+v_\perp^2/2}\right)=\frac{k^2}{2}g\,, \tag{5}$$

where, $\int_L$ means the integral is along the Landau route and the following normalization and definition are adopted: $v=v/v_{ti}$, $k=k\rho_i$, $\zeta\equiv qR\omega/v_{ti}$, and $\tau\equiv q_iT_e/\left(eT_i\right)$. Equation (5) describes the dynamics of ZFs in the large aspect ratio circular geometry where the plasma is collisionless but the trapped particle effect is not considered. When $T_e<<T_i$, only the ion response contribute the zonal flow dynamics. We have studied this case recently.[9] Here, we will repeat some derivations for the sake of clarity and completeness, but focus on the behavior of different types of eigenmode at finite τ.

3. Analytical and Numerical Results

Firstly, we consider the limit of drift kinetic model, where $k\to 0$ but $k\hat{\phi}$ is finite. In another word, k is of arbitrary low order. In this case, we retain the $O\left(k^2\right)$ terms in the LHS of Eq. (4) and then get

$$G(\zeta)\equiv\frac{1}{q^2}+\frac{1}{2}-\frac{(1+\tau)}{2\zeta^2}+\left(\zeta^2+1+\tau+\frac{1+\tau}{2\zeta^2}\right)\left[1+\zeta Z(\zeta)\right]=0 \tag{6}$$

where $Z(\zeta)$ is the well known plasma dispersion function. In the following, we will analytically solve Eq. (6) in different limits of ζ before numerical results are given.

(a) the standard GAM. For $|\zeta|>1$, asymptotically expanding $Z(\zeta)$, i.e. $Z(\zeta)=i\pi^{1/2}\sigma e^{-\zeta^2}-1/\zeta-1/\left(2\zeta^3\right)-3/\left(4\zeta^5\right)-...$, and retaining the leading terms, we get the asymptotic form of Eq. (6),

$$G_A(\zeta)\equiv\frac{1}{q^2}-\frac{1}{\zeta^2}\left(\frac{7}{4}+\tau\right)-\frac{1}{\zeta^4}\left(\frac{23}{8}+\tau\right)+i\pi^{1/2}\zeta^3e^{-\zeta^2}=0\,. \tag{7}$$

Under the assumption of $\gamma<<\omega_r$, the frequency of GAM are analytically obtained,

$$\omega_{GAM}^2=\left(\frac{7}{4}+\tau\right)\frac{v_{ti}^2}{R^2}\left[1+\frac{46+16\tau}{(7+4\tau)^2q^2}\right] \tag{8a}$$

$$\gamma_{GAM}=-\frac{\pi^{1/2}}{2}\left(\frac{7}{4}+\tau\right)^2\exp\left(-\frac{23+8\tau}{14+8\tau}\right)\frac{v_{ti}}{R}q^5\exp\left[-\left(\frac{7}{4}+\tau\right)q^2\right]. \tag{8b}$$

Here, the assumption of high q is used and only the leading terms with respect to q are retained. So, this dispersion relation is expected to be enough accurate only when q is high

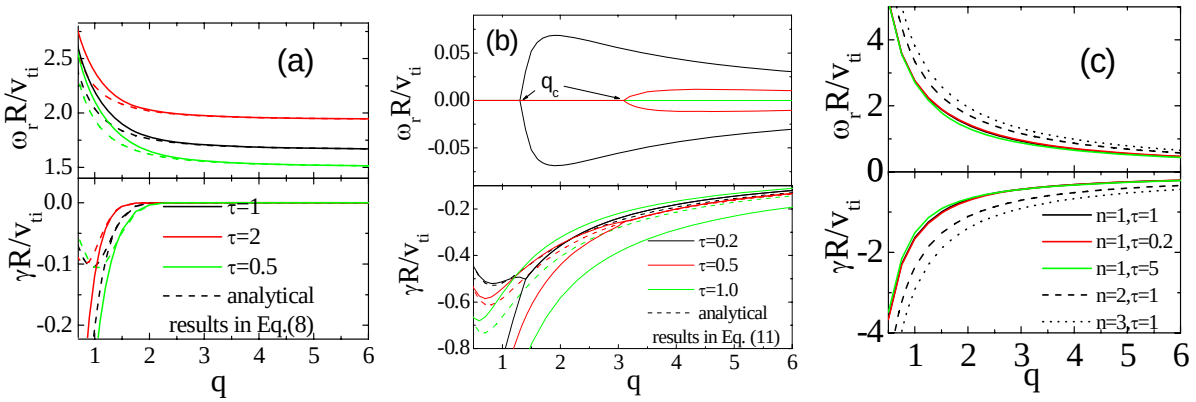

Fig.1. The frequency and damping rate of standard GAM (a), low frequency eigenmode (b), and ISW-like eigenmodes (c) as functions of q for different τ.

enough. Regarding $1/qR$ as $k_{//}$, this kind of transit time magnetic pumping (TTMP) damping has the same resonance condition as the Landau damping. The damping rate varies as the scaling of $q^5 \exp\left[-(7/4+\tau)q^2\right]$, so the standard GAM is weakly damped in the high q edge region. As τ increases, the frequency of GAM increases and then the damping is weakened. It is because the electron parallel flow (adiabatic response to the $m=1$ potential) partially compensates the divergence of the $m=0$ $\mathbf{E}\times\mathbf{B}$ flow but does not induce ion Landau-type damping.

When q is low, more expansion terms may be required in Eq.(7) for results with enough precision, which, however, makes the analytical evaluation is hard to carry out. So it is more convenient to direct numerically solve Eq.(6). Numerical results for the frequency and damping rate of the standard GAM are given in Fig.1(a). It is shown that the analytical formulae (8) are well consistent with numerical results in the high q region. Although the discrepancy grows at lower q, formula (8a) still can give an approximate dependence of the GAM frequency on q.

(b) the low frequency eigenmode. The standard GAM has a relative high frequency $\omega > v_{ti}/qR$ for all q. Here, we will identify a branch of low frequency eigenmode. For $\zeta \le 1$, $Z(\zeta) = -2\zeta\left(1-2\zeta^2/3+4\zeta^4/15+...\right)+i\pi^{1/2}\exp\left(-\zeta^2\right)$. Substituting it into Eq. (6) and retaining the leading terms, we get

$$G_S(\zeta) \equiv \frac{1}{q^2}+\frac{1}{2}-\frac{\zeta^2}{3}(1+4\tau)+i\frac{\pi^{1/2}}{2}\left[\frac{(1+\tau)}{\zeta}+(1+\tau)\zeta\right]=0 \qquad (9)$$

Here, $\exp(-\zeta^2)$ is also expanded with its power series. Substituting $\zeta=\zeta_r+i\zeta_i$ into Eq. (9), we get

$$i\left[\frac{\pi^{1/2}}{2}(1+\tau)+\left(\frac{1}{q^2}+\frac{1}{2}\right)\zeta_i-\frac{\pi^{1/2}}{2}(1+\tau)\zeta_i^2+\frac{\zeta_i^3}{3}(1+4\tau)+\zeta_r^2\left(\frac{\pi^{1/2}}{2}(1+\tau)-\zeta_i(1+4\tau)\right)\right]$$

$$+\zeta_r\left[\frac{1}{q^2}+\frac{1}{2}-\pi^{1/2}(1+\tau)\zeta_i+\left(\zeta_i^2-\frac{\zeta_r^2}{3}\right)(1+4\tau)\right]=0 \qquad (10)$$

An obvious solution is $\zeta_r=0$. Substituting $\zeta_r=0$ and omitting the $O(\zeta_i^3)$ terms in the imaginary part of the LHS of Eq.(10), we get the eigenfrequency of zonal flow

$$\omega_{lf}=0 \qquad (11a)$$

$$\gamma_{lf}=-\frac{\nu_{ti}}{qR}\left[\sqrt{1+\frac{1}{(1+\tau)^2\pi}\left(\frac{1}{2}+\frac{1}{q^2}\right)^2}-\frac{1}{(1+\tau)\sqrt{\pi}}\left(\frac{1}{2}+\frac{1}{q^2}\right)\right] \qquad (11b)$$

However, results in formulae (11a) and (11b) are not always valid for any q. In fact, the $1/q^2-G(0+i\zeta_i)$ has a minimum value in the half-space $\zeta_i<0$. If this minimum value, $c_{\min}$, is negative, Eq. (6) has a rigid zero frequency solution in the whole q region. However, if $c_{\min}>0$, the rigid zero frequency solution is valid only for $q<c_{\min}^{-1/2}$ and a finite real frequency is required for higher q. Figure 2 give the plot of $1/q^2-G(0+i\zeta_i)$ as functions of ζ_i for different τ. We can see that the $c_{\min}$ become positive when $\tau<0.55$.

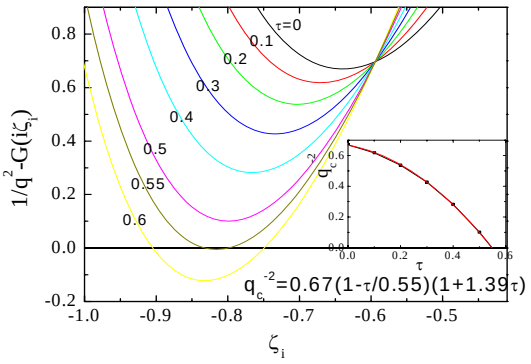

Fig. 2. $1/q^2-G(0+i\zeta_i)$ *vs.* ζ_i *for different* τ *(and* q_b *vs.* τ *)*

Numerical results for the low frequency eigenmode are also given in Fig.1(b). Obviously, at a low τ, a bifurcation occurs at a critical q, q_c. For $q<q_c$, two modes have rigid zero frequencies and different damping rates; while, for $q>q_c$, they transfer into two modes with the same damping rate and opposite nonzero frequencies. However, when the electron temperature is so high as to $\tau\geq 0.55$, two eigenmodes with rigid zero frequency exists for all q. The real frequency of the mode can be roughly described as follows

$$\begin{cases}\omega_{lf}\approx\pm 0.2\dfrac{\nu_{ti}}{qR}\sqrt{\left[1-\left(\dfrac{\tau}{0.55}\right)^2\right]\left[1-\left(\dfrac{q_c}{q}\right)^2\right]} & for\quad \tau<0.55\ and\ q>q_c\\ \omega_{lf}=0 & otherwise\end{cases} \qquad (11c)$$

where $q_c^{-2}=0.67(1-\tau/0.55)(1+1.39\tau)$. In the whole q and τ region, the damping rate of the relative weakly damped mode is well described by the analytical formula (11b).

c) ***the ISW-like eigenmodes.*** In this case, $|\zeta| >> 1$ and $|\zeta_r| \sim |\zeta_i|$, therefore the governing equation of ζ_r and ζ_i strongly coupled. The oscillating exponential term, in Eq.(7) dominates these modes. Therefore, it is expected that finite τ hardly influence this series of modes. The dispersion relation we obtained for $\tau = 0$ [9] is still valid, that is

$$\omega_{ISW-like} \approx \pm \frac{v_{ti}}{qR} \sqrt{n\pi + \ln q + \varepsilon_1} \tag{12a}$$

$$\gamma_{ISW-like} \approx -\frac{v_{ti}}{qR} \sqrt{n\pi - \ln q + \varepsilon_2} \tag{12b}$$

where ε_1 and ε_2 are two fitting parameters. It is noted that the above assumptions we adopted may induce the validity limit of n and q. Fortunately, however, Eqs.(12) can fit the numerical results for the three lowest damped branches of ISW-like eigenmodes, with $n = 1, 2, 3$, $\varepsilon_1 = 4.41, 4.77, 5.03$ and $\varepsilon_2 = -0.30, -0.69, -0.92$, respectively. Figure 1(c) shows these modes, as well as the $n = 1$ mode for different τ's. Indeed, the ISW-like mode is hardly influenced by finite τ. We call them the ISW-like eigenmodes because their frequencies are inverse proportional to q. In fact, they can be considered as result of the coupling of harmonic ion transit flows to the poloidal $\mathbf{E} \times \mathbf{B}$ flow. Here, since the oscillation of density mostly comes from the ion transit dynamics, the series of modes is strong damped.

The effect of finite orbit width, $k\rho_i q$, can enhance the collisionless damping of the standard GAM, which is confirmed by Sugama and Watanabe.[8] This enhanced damping was understood as an additional damping at the resonant condition $v_{//} \sim \omega qR/2$. Retaining the second order Bessel function in Eq. (5), we obtain

$$\begin{aligned} &Q_2 P_0 + Q_1(P_1 + \tau P_0) + \frac{1}{4} Q_0 (P_2 + 2\tau P_1) + \frac{k^2 q^2}{4} \left[(R_3 - Q_3) P_0 + (R_2 - Q_2)(2P_1 + \tau P_0) \right. \\ &\left. + \frac{3}{2}(R_1 - Q_1)(P_2 + \tau P_1) + \frac{1}{2}(R_0 - Q_0)\left(P_3 + \frac{3}{2}\tau P_2 \right) + \frac{1}{16}(R_{-1} - Q_{-1})(P_4 + 2\tau P_3) \right] = \frac{1}{q^2} g \end{aligned}, \tag{13}$$

where $\mathrm{P}_n = \int dv_\perp^2 \exp(-v_\perp^2) J_0^2(kv_\perp) v_\perp^{2n}$, $Q_n \equiv \int_L \frac{dv_{//}}{\pi^{1/2}} \exp(-v_{//}^2) \frac{v_{//}^{2n}}{\omega^2 - v_{//}^2}$, and $R_n = \frac{1}{4} Q_n(\omega/2)$.

Obviously, there exists the competition between R_n (resonance at $v_{//} \sim \omega qR/2$) and Q_n (resonance at $v_{//} \sim \omega qR$) in the terms introduced by finite $k\rho_i q$. In fact, as $k\rho_i q$ increases, a series of resonance at $v_{//} \sim \omega qR/n$ becomes effective. Figure 3 shows the real frequencies and damping rates for the standard GAM as functions of $k\rho_i$ and q. It is seen that, although the collisionless damping is enhanced for all q as $k\rho_i$ increases, the enhancement is especially strong in the region near $q \sim 2$. As a result, the damping rate of the GAM with finite spectrum width is probably not monotonic as q varies.

Figure 4 shows the results for the low/zero frequency eigenmode at $\tau = 1$ from Eq. (13). It is found that the collisionless damping of this mode is slightly weakened by finite k. The finite orbit width effect also changes the bifurcation condition. Even at $\tau = 1$, the mode

require a finite real frequency when $k\rho_i q$ is large enough, as shown in Fig. (4). However, as $k\rho_i q$ increases, the term with higher order Bessel function may be important in Eq.(6), especially for the low frequency eigenmode with $\omega_r << \gamma$. Therefore, more careful treatment will be made in future.

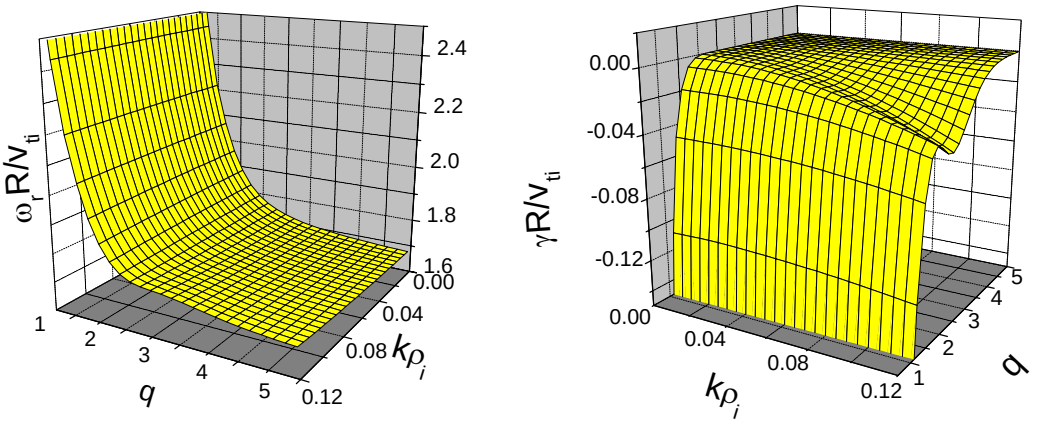

Fig. 3. Real frequency and damping rate for the standard GAM at $\tau = 1$ *as functions of* $k\rho_i$ *and* q.

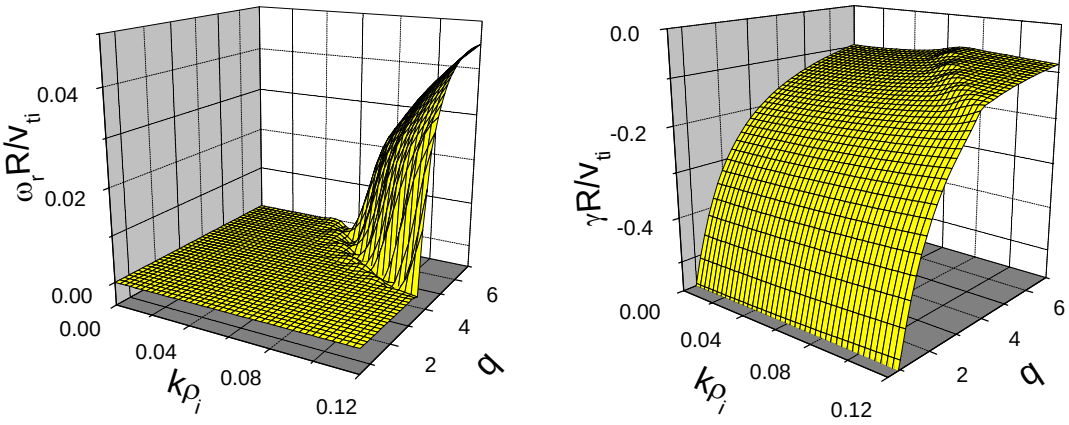

Fig. 4. Real frequency and damping rate for the low frequency eigenmode at $\tau = 1$ *as functions of* $k\rho_i$ *and* q

4. Discussion and Summary

Here, we consider the collisionless case, but the trapped ion effects have not been included. Lebedev et al [10] have also investigated the relaxation dynamics of the radial electrical field in the plateau, where an infinite series of eigenmode, even the bifurcation of the low frequency branch are found. However, the authors paid more attention on the GAM oscillation which is most weakly damped and has left the low frequency eigenmode for future studies in some sense. The problem of zero-frequency zonal flow was elegantly solved by Rosenbluth and Hinton [6] as an initial value problem. The importance of the zero-frequency zonal flows ($|\omega = 0|$ in the collisionless limit) has been well known, but the zero-real-frequency branch of Fig. 1(b) has the relevance as well. If we consider the case in the plateau regime, the damping rate of this new branch is in the same order of magnitude in

comparison with that of the Rosenbluth-Hinton zonal flow. Even in the banana regime, its damping rate is larger than that of the latter by a factor, not by an exponential difference. Thus, a substantial energy from turbulence could be injected into this new branch of $\omega_r = 0$ in comparison with the standard zero frequency zonal flows.

In summary, a series of GAM eigenmodes which includes the standard GAM, a branch of low frequency mode and infinite ISW-like modes is reported. Eigenfrequencies of these modes are obtained analytically from a linear gyrokinetic model in collisionless toroidal plasmas with a nearly constant electrostatic potential around a magnetic surface. The ISW-like modes has a frequency spectrum roughly with a progression of $\sqrt{n\pi}$ times the transit frequency and strongly damped. The low frequency eigenmode oscillates with a finite frequency in the region of low τ and high q, but has a rigid zero frequency elsewhere. This low frequency mode relaxes on time scaling with the order of transit frequency $v_{ti}/(qR)$. The effect of finite orbit width on the modes has also been briefly discussed. Considering different damping rates of these modes, only a few (the least damped and/or the most excited) modes may play a role in the turbulence dynamics.

ACKNOWLEDGEMENT

One of the authors (ZG) is grateful for the hospitality by many staff members during his visit at the National Institute for Fusion Science, Japan. This work is supported partly by the JSPS-CAS Core University Program on Plasma and Nuclear Fusion, and partly by National Science Foundation of China, Grants No. 10405014.

[1] DIAMOND, P. H., et al., Plasma Phys. Control. Fusion **47** (2005) R35.
[2] WINSOR, N., JOHNSON, J. L., and DAWSON, J. M., Phys. Fluids **11**(1968) 2448.
[3] FUJISAWA, A., Plasma Phys. Contr. Fusion **48** (2006) S31
[4] ITOH, K., et al., Phys. Plasmas **13** (2006) 055502.
[5] ITOH, K., ITOH, S.-I., and FUKUYAMA, A., *Transport and structural Formation in Plasmas,* IOP, England, 1999, pp235-239.
[6] ROSENBLUTH, M. N. and HINTON, H. L., Phys. Rev. Lett. **80** (1998) 724.
[7] WATARI, T. et al., Phys. Plasmas **12** (2005) 062304.
[8] SUGAMA, H. and WATANABE T.-H., Phys. Plasmas **13**(2006) 012501.
[9] GAO, Z., ITOH, K., SANUKI, H., and DONG, J.Q., Phys. Plasmas **13**(2006) in press.
[10] LEBEDEV, V. B., et al., Phys. Plasmas **3** (1996) 3023